scientific reports

OPEN

Multiwaves, breathers, lump and other solutions for the Heimburg model in biomembranes and nerves

Dilber Uzun Ozsahin[1,2 ✉], Baboucarr Ceesay[3,4], Muhammad Zafarullah baber[3], Nauman Ahmed[3,10], Ali Raza[5,10], Muhammad Rafiq[6,10], Hijaz Ahmad[7,8,10,11], Fuad A. Awwad[9] & Emad A. A. Ismail[9]

In this manuscript, a mathematical model known as the Heimburg model is investigated analytically to get the soliton solutions. Both biomembranes and nerves can be studied using this model. The cell membrane's lipid bilayer is regarded by the model as a substance that experiences phase transitions. It implies that the membrane responds to electrical disruptions in a nonlinear way. The importance of ionic conductance in nerve impulse propagation is shown by Heimburg's model. The dynamics of the electromechanical pulse in a nerve are analytically investigated using the Hirota Bilinear method. The various types of solitons are investigates, such as homoclinic breather waves, interaction via double exponents, lump waves, multi-wave, mixed type solutions, and periodic cross kink solutions. The electromechanical pulse's ensuing three-dimensional and contour shapes offer crucial insight into how nerves function and may one day be used in medicine and the biological sciences. Our grasp of soliton dynamics is improved by this research, which also opens up new directions for biomedical investigation and medical developments. A few 3D and contour profiles have also been created for new solutions, and interaction behaviors have also been shown.

Keywords Heimburg model, Hirota bilinear method, Soliton solutions, Physical representation

Advances in nonlinear partial differential equations (NLPDEs), a powerful tool for many interdisciplinary investigations, have made it possible to investigate complex physical phenomena in disciplines like fluid science, control theory, hydrodynamics, geochemistry, optical science, and plasma[1,2]. In biological systems, soliton production and propagation in neurons and biomembranes is crucial[3,4]. Accurate NLPDE solutions are critical for comprehending the complex mechanisms that govern these procedures.

The recent development of novel techniques for obtaining soliton solutions from NLPDEs has significantly improved our ability to recognize and investigate these occurrences. Finding exact soliton solutions proved to be an extremely successful application of the Hirota bilinear technique[5,6]. Among the applications of this method that have proved successful include the analysis of nonlinear Schrödinger equations, integrable systems, and optical fibers[7,8]. Regarding the mechanical systems that support nerves and biomembranes, the Heimburg model offers essential details. The nerve axon is portrayed in the model as a cylinder-shaped biomembrane that changes

[1]Department of Medical Diagnostic Imaging, College of Health Sciences, Sharjah University, Sharjah, United Arab Emirates. [2]Research Institute for Medical and Health Sciences, University of Sharjah, Sharjah, United Arab Emirates. [3]Mathematics and Statistics Department, The University of Lahore, Lahore, Pakistan. [4]Mathematics Unit, The University of The Gambia, Sere Kunda, The Gambia. [5]Department of Mathematics, Govt. Maulana Zafar Ali Khan Graduate College Wazirabad, Punjab Higher Education Department (PHED), Lahore 54000, Pakistan. [6]Department of Mathematics, Faculty of Science and Technology, University of Central Punjab, Lahore, Pakistan. [7]Section of Mathematics, International Telematic University Uninettuno, Corso Vittorio Emanuele II, 39,00186 Roma, Italy. [8]Near East University, Operational Research Center in Healthcare, TRNC Mersin 10, Nicosia, 99138, Turkey. [9]Department of Quantitative analysis, College of Business Administration, King Saud University, P.O. Box 71115, 11587 Riyadh, Saudi Arabia. [10]Department of Computer Science and Mathematics, Lebanese American University, Beirut, Lebanon. [11]Center for Applied Mathematics and Bioinformatics, Gulf University for Science and Technology, Mishref, Kuwait. ✉email: dozsahin@sharjah.ac.ae

from a fluid to a gel structure at a specific temperature below average. The soliton dynamics in this framework provide crucial information regarding the nature of nerve impulses, which makes it crucial to understand.

The Hirota bilinear technique[9,10] is utilized in this investigation to evaluate the soliton production and propagation in biomembranes and neurons employing the Heimburg model. Using this technique, we can obtain precise soliton solutions and learn more about how electromechanical pulses behave differently within nerves. This analytical method illuminates the basic concepts that underlie biological systems by studying the intricate interactions between biomembranes and solitons. By combining the power of the Hirota bilinear technique with the understanding gained from the Heimburg model, this study contributes to a clearer understanding of the complicated dynamics of soliton occurrences in biological systems. The findings might influence a variety of fields, such as biophysics, neuroscience, and bioengineering, and they might hasten the development of therapeutic interventions and bio-inspired technology.

The Heimburg model is an integrable differential equation, there is no general technique to solve these equation. Zhang et al. proposed the symbol calculation method based on neural networks to obtained the exact analytical solutions for the NLPDEs. The Bilinear residual network method is used to obtained the exactly explicit solutions for the nonlinear evolution equations[11]. For the first time bilinear neural network model is used to get the exact analytical solution for the reduced p-gBKP equation[12], the different types of soliton solutions are also constructed by using this technique for the (3+ 1)-dimensional Jimbo-Miwa equation[13]. The new test functions Fractal solitons, arbitrary function solutions, exact periodic wave, breathers, generalized lump solutions, classical lump solutions and rogue waves are constructed[14–16], and the interference wave and the bright and dark soliton are also constructed via bilinear residual network method[17,18].

Khatun, et al., worked on the couple modified equal-width and Boussinesq equations constructed the soliton solutions by using the Sine-Gordon expansion[19]. Arefin, et al., investigated the closed form travelling wave solution for the non-linear evolution equations using the two-variable $(G'/G, 1/G)$-expansion method[20]. Zaman, et al., explored soliton wave propagation for the nonlinear coupled type Boussinesq-Burger (BB) and coupled type Boussinesq equations via extended tanh-function method[21]. Pan, et al., worked on the derivative nonlinear Schrödinger equation to construct the optical soliton solutions by using the extended modified auxiliary equation mapping technique[22]. Seadawy et al., used the extended modified auxiliary equation mapping to explored the optical solitons for the perturbed nonlinear fractional Schrödinger equation[23] and the integrable improved perturbed nonlinear Schrödinger equation with type of Kerr law nonlinearity[24,25]. Cheemaa et al., analyzed the soliton solutions for the nonlinear modified Korteweg-de Vries equation using the auxiliary equation mapping method[26].

A mathematical method utilised in the study of nonlinear systems and soliton theory is the Hirota bilinear transformation. It was developed by Ryogo Hirota to explore soliton of nonlinear equations, particularly PDEs that admit soliton solutions - localised, stable, and often interacting wave-like structures. The Hirota bilinear transformation's main goal is to express NLPDEs in a bilinear form. This bilinear form facilitates the investigation of the underlying dynamics and makes it possible to develop multi-soliton solutions. Once the soliton equation is expressed in bilinear form, solutions can be obtained by solving the resulting system of bilinear equations. The bilinear form facilitates the study of multi-soliton solutions, their interactions, and the underlying dynamics of the original soliton equation. The solutions obtained through the Hirota bilinear transformation provide insights into the behavior of solitons in the system described by the original equation. These solutions often exhibit interesting phenomena such as soliton collisions, fusion, and fission. In travelling wave theory, the application of asymptotic techniques helps to fully comprehend the dynamics of solitons by capturing their leading-order behaviour. This method also forms the basis for numerical simulations, which direct and validate computational studies on solitons in NLPDEs. In general, travelling wave theory shows to be an effective and adaptable method for understanding the complex nature of soliton occurrences in a range of nonlinear systems. So, under considered method is more effective our the other analytical techniques because the special types of solitons are generated. This approach is provided us the special types of soliton solutions such as, breather wave, Lump wave, multi-wave, mixed wave, M-shape, rough wave, one kink, two kink, periodic cross kink and many others. But method are provided us only hyperbolic, trigonometric and rational wave solutions.

But in this study we use hirota bilinear method which is efficient technique that will provided us the different form of solitons like, breather wave, lump wave, multiwave, M-shapes and many other interactions. The different types of soliton solutions for the Heimburg model. These solutions have many applications in biomembranes and nerves can be studied using this model. The Hirota bilinear transformation is used to construct the homoclinic breather waves, interaction via double exponents, lump waves, multi-wave, mixed type solutions, and periodic cross kink solutions. These solution have there significance in the dynamical study of biomembranes and nerves which also opens up new directions for biomedical investigation and medical developments. The soliton are plotted in 3D and contour profiles for new solutions, and interaction behaviors have also been shown. There plots are show the Breather waves, lump waves, multiple wave, periodic cross kink solutions. These plots have the physical significance in the energy propagation patterns inside the biomembranes. It's crucial to remember, nevertheless, that generating real graphical representations could call for specific tools and software. A breather wave is an oscillating or pulsing localized disturbance that moves through the membrane. Seek for a graph that illustrates a spike or disturbance that occurs at a specific point along the membrane and then vanishes. Over time, the wave's amplitude could change. A concentrated, non-dispersive energy package passing across the membrane is represented as a lump wave. Imagine a wave that propagates through the membrane without greatly expanding or altering form, all the while maintaining its amplitude and shape. The coexistence of many waves in the membrane at various frequencies and amplitudes is referred to as multiple waves. Look for a graph that shows several waveforms interacting with one another inside the membrane, each with a different frequency and amplitude. These plot have the significance in the theoretical and experiential study of nonlinear Heimburg model.

The nonlinear Heimburg model will be introduced in "An overview of the model" to provide a theoretical basis for our study. "An overview of the method" will describe the Hirota bilinear method, which we will use to conduct our analysis. "Application of the method on the Heimburg model" will apply the Hirota bilinear method to the Heimburg model, extracting exact soliton solutions, and examining their properties. "Graphical presentations" will deal with the findings by presenting them in graphical illustrations and in "Conclusion" we conclude on our findings.

An overview of the model

Numerous mathematical models have been used to examine the propagation of electrical signals in nerve axons in great detail[27–29]. Action potential dynamics have been better understood thanks to the Hodgkin-Huxley model[30], which is based on the reaction-diffusion equation. The more straightforward model put forth by FitzHugh and Nagumo has also provided a more manageable framework for studying pulse propagation[30]. These models, however, do not take into consideration how nerve conduction works mechanically. We offer the Heimburg model to fill up this knowledge gap, which integrates electrical and mechanical dynamics to provide a more comprehensive comprehension of sound transmission in nerve axons. In the Heimburg model, proteins are viewed as resistors and membranes as capacitors in an electrical circuit that represents the nerve axon. With the use of this conceptualization, we may define the voltage fluctuation across the neuron membrane as a propagating action potential[31]. Along the nerve axon, a voltage pulse is created by the ion currents the membrane produces[31]. We take into account lateral density excitations within a one-dimensional cylindrical nerve axon to take the mechanical elements into account. The following equation can be used to describe how sound propagates via nerve axons without dispersion[1]

$$\frac{\partial^2 \Delta\rho^A}{\partial\tau^2} = \frac{\partial}{\partial z}\left(c^2 \frac{\partial \Delta\rho^A}{\partial z}\right), \tag{1}$$

where τ represents time, z denotes the position along the nerve axon, and $\Delta\rho_A$ is the difference in nerve axon area density between the gel state ρ_A and the fluid state ρ_A^0. The sound velocity $c = \sqrt{\frac{1}{\kappa_s^A \rho^A}}$ depends on density and is determined by the properties of the nerve axon. Here, κ^A represents a constant related to the hydrodynamic Euler equation.

We add a frequency-dependent sound velocity that permits the generation of solitons to the Heimburg model in order to account for dispersion and nonlinear effects. To accomplished this, the sound speed equation was modified[1] as follows:

$$c^2 = c_0^2 + \alpha\Delta\rho^A + \beta\left(\Delta\rho^A\right)^2, \tag{2}$$

where c_0 represents the velocity of small amplitude sound, $\alpha < 0$ and $\beta > 0$ are constants, and $\Delta\rho^A$ is the difference in density between the gel and fluid states. We include a higher-order term $-h\frac{\partial^4 \Delta\rho^A}{\partial z^4}$ to Eq. (1) to account for mechanical dispersion. As a result, the following equation describes how sound travels through nerve axons,

$$\frac{\partial^2 \Delta\rho^A}{\partial\tau^2} = \frac{\partial}{\partial z}\left(c_0^2 + \alpha\Delta\rho^A + \beta(\Delta\rho^A)^2\right)\frac{\partial \Delta\rho^A}{\partial z} + u\frac{\partial^2 \Delta\rho^A}{\partial z^2}\frac{\partial \Delta\rho^A}{\partial\tau} - h\frac{\partial^4 \Delta\rho^A}{\partial z^4}, \tag{3}$$

where $c_0 = \frac{1}{K_s^A \rho_0^A}$, $\alpha = -\frac{1}{K_s^A (\rho_0^A)^2}$, and $\beta = \frac{1}{K_s^A (\rho_0^A)^3}$.

Consider the dimensionless variables u, x, and t given as: $\upsilon = \frac{\Delta\rho^A}{\rho_0^A}$, $x = \frac{c_0 z}{\sqrt{h}}$, $t = \frac{c_0^2 \tau}{\sqrt{h}}$

Using these new variables, we arrive at the dimensionless density-wave equation from Eq. (3) as follows[1]:

$$\frac{\partial^2 \upsilon}{\partial t^2} = \frac{\partial}{\partial x}\left(\left(1 + b_1\upsilon + b_2\upsilon^2\right)\frac{\partial \upsilon}{\partial x}\right) - \frac{\partial^4 \upsilon}{\partial x^4} + m_2\frac{\partial^3 \upsilon}{\partial x^2 \partial t}, \tag{4}$$

with $m_2 = \frac{u}{\sqrt{h}}$, $b_2 = \frac{(\rho_0^A)^2}{c_0^2}\beta$, and $b_1 = \frac{\rho_0^A}{c_0^2}\alpha$. Equation (4) is our required Heimburg model that we used in this paper. In the next section, we give an overview about the Hirota bilinear method.

An overview of the method

This section we outline the method used in the formation of the model for this paper. We start by first stating the general form of the nonlinear partial differential equation (NLPDE)

$$W(\upsilon, \upsilon_x, \upsilon_t, \upsilon_{xx}, \upsilon_{xt}, ...) = 0, \tag{5}$$

in this case, W is a polynomial in $\upsilon(x, t)$. The following are the main phases in this method:

Phase 1: Consider the following transformation[32–35]:

$$\upsilon(x, t) = \lambda(\eta), \quad \eta = x - m_1 t, \tag{6}$$

where m_1 denotes the density pulse's velocity. Equation (6) converts Equation (5) into the following form:

$$U(\lambda, \lambda', \lambda'', \lambda''', ...) = 0, \tag{7}$$

for polynomial U in $\lambda(\eta)$ having derivatives $\lambda^{'}(\eta)$, $\lambda^{''}(\eta)$, $\lambda^{'''}(\eta)$, etc is twice integrable differential equation.

Phase 2: Assume Eq. (7) has a solution of the form:

$$\lambda = \frac{f'(\eta)}{f(\eta)}, \tag{8}$$

where $f(\eta)$ is an unidentified function to be determined for our required solutions.

Phase 3: In this phase, we will determine λ', λ'', λ''', ..., of Eq. (8) and substitute them into Eq. (7) to obtain an equation in terms of $f(\eta)$ and its derivatives upto the fifth order. We then integrate the resulting equation twice to to obtained our Bilinear form.

Phase 4: The numerous wave structures under consideration are now inserted into the Bilinear equation generated in phase (3). Then, in each case, we expand, simplify, and collect like terms and equate them to 0. Finally, in each situation, we solve the set of equations to obtain the suitable solutions.

Application of the method on the Heimburg model

In this section, we used the previously stated stages to determine the various soliton generation and propagation in biomembranes and nerves for the Heimburg model.

We begin by considering Eq. (4), the dimensionless density-wave model. We now transform Eq. (4) to an ODE using the transformation $\upsilon(x, t) = \lambda(\eta)$, with $\eta = x - m_1 t$, where m_1 is the velocity of the density pulse to obtain:

$$m_1\lambda'' - b_1(\lambda')^2 - b_2\lambda(\lambda')^2 - \lambda'' - b_1\lambda\lambda'' - b_2\lambda^2\lambda'' + \lambda'''' + m_1 m_2\lambda''' = 0. \tag{9}$$

Next we transform Eq. (9) from an ODE to a bilinear form using the the transformation

$$\lambda = \frac{f'(\eta)}{f(\eta)}, \tag{10}$$

Substituting Eq. (10) into the Eq. (9) and integrating twice we obtained the bilinear form such as

$$-2(b_2 - 6)f'^3 - 3ff'\left(b_1 f' + 6f'' + 2m_1 m_2 f'\right) + 6f^2\left(f''' + m_1 m_2 f'' + \left(m_1^2 - 1\right)f'\right) = 0. \tag{11}$$

We now substitute the different wave structures we are studying into Eq. (11). Then, in each case, we expand, simplify, and collect like terms and equate them to 0. Finally, in each situation, we solve the set of equations to obtain the suitable solutions.

1. Homoclinic breather: we find some solutions using the homoclinic breather transformation such ass[10,36]:

$$f = \exp\left(-v(d_1\eta + d_2)\right) + w_1 \exp\left(v(d_3\eta + d_4)\right) + w_2 \cos\left(v(d_5\eta + d_6)\right). \tag{12}$$

Substituting Eq. (12) and its derivatives to the third order into Eq. (9), simplifying and combining like terms using exponential, trigonometric, and exponential-trigonometric functions, and setting each of the resulting expressions to 0, we can determine the values of some of the parameters as follows:

Family 1: the constant values are taken as $d_1 = -d_3$, $d_5 = -\frac{d_3\sqrt{3m_2^2 m_1^2 + 4m_1^2 - 4}}{m_1 m_2}$, $v = \frac{m_1 m_2}{2d_3}$, $b_1 = \frac{2(m_2^2 m_1^2 - 3m_1^2 + 3)}{m_1 m_2}$, $b_2 = \frac{6(m_2^2 m_1^2 - m_1^2 + 1)}{m_1^2 m_2^2}$, while w_1, w_2, d_2, d_4, d_6 are the free parameters.

Substituting them in Eq. (12) and then in Eq. (10) the result is, obtained such as

$$\lambda_{1,1}(\eta) = \frac{\frac{1}{2}m_1 m_2 e^{-\frac{m_1 m_2(d_2 - d_3\eta)}{2d_3}} + \frac{1}{2}m_1 m_2 w_1 e^{\frac{m_1 m_2(d_3\eta + d_4)}{2d_3}} + \frac{1}{2}\sqrt{3m_2^2 m_1^2 + 4m_1^2 - 4}\, w_2 \sin(G)}{e^{-\frac{m_1 m_2(d_2 - d_3\eta)}{2d_3}} + w_1 e^{\frac{m_1 m_2(d_3\eta + d_4)}{2d_3}} + w_2\cos(G)}, \tag{13}$$

where $G = \frac{m_1 m_2\left(d_6 - \frac{d_3\eta\sqrt{3m_2^2 m_1^2 + 4m_1^2 - 4}}{m_1 m_2}\right)}{2d_3}$. The breather wave solution to Eq. (4) is gained as:

$$\upsilon_{1,1}(x, t) = \frac{\sqrt{m_1^2(3m_2^2 + 4) - 4}\, w_2 e^{\frac{m_1 m_2(d_3(m_1 t - x) + d_2)}{2d_3}} \sin(K) + m_1 m_2\left(w_1 e^{\frac{(d_2 + d_4)m_1 m_2}{2d_3}} + 1\right)}{2\left(w_2 e^{\frac{m_1 m_2(d_3(m_1 t - x) + d_2)}{2d_3}} \cos(K) + w_1 e^{\frac{(d_2 + d_4)m_1 m_2}{2d_3}} + 1\right)}, \tag{14}$$

where $K = \frac{d_6 m_1 m_2}{2d_3} + \frac{1}{2}\sqrt{m_1^2(3m_2^2 + 4) - 4}(m_1 t - x)$.

Family 2: the constant values are taken as $w_1 = 0$, $d_1 = \frac{\sqrt{m_1^2(9m_2^2 + 8) - 8} - 3m_1 m_2}{4v}$, $d_5 = \frac{\sqrt{\frac{m_1^2 m_2^2\left(-(9m_2^2 + 4)m_1^2 + 3\sqrt{m_1^2(9m_2^2 + 8) - 8}m_2 m_1 + 4\right)}{v^2}}}{2\sqrt{2}m_1 m_2}$, $b_1 = -8m_1 m_2$, $b_2 = -\frac{3\left((3m_2^2 - 4)m_1^2 + \sqrt{m_1^2(9m_2^2 + 8) - 8}m_2 m_1 + 4\right)}{2(m_1^2 - 1)}$ while w_2, d_2, d_3, d_4, d_6 are the free parameters.

Substituting them in Eq. (12) and then in Eq. (10) the result is, obtained such as

$$\lambda_{1,2}(\eta) = \frac{\frac{1}{4}\left(3m_1m_2 - \sqrt{m_1^2(9m_2^2+8)-8}\right)e^{-v\left(d_2 + \frac{\eta\left(\sqrt{m_1^2(9m_2^2+8)-8}-3m_1m_2\right)}{4v}\right)} - J\sin(G)}{e^{-v\left(d_2 + \frac{\eta\left(\sqrt{m_1^2(9m_2^2+8)-8}-3m_1m_2\right)}{4v}\right)} + w_2\cos(G)}. \tag{15}$$

The breather wave solution to Eq. (4) is gained as:

$$\upsilon_{1,2}(x,t) = \frac{\frac{1}{4}\left(3m_1m_2 - \sqrt{m_1^2(9m_2^2+8)-8}\right)e^{\frac{1}{4}\left(\sqrt{m_1^2(9m_2^2+8)-8}-3m_1m_2\right)(m_1t-x)-d_2v} - J\sin(G(x-m_1t))}{e^{\frac{1}{4}\left(\sqrt{m_1^2(9m_2^2+8)-8}-3m_1m_2\right)(m_1t-x)-d_2v} + w_2\cos(G(x-m_1t))}, \tag{16}$$

where $G = v\left(d_6 + \frac{\eta\sqrt{\frac{m_1^2m_2^2\left(-(9m_2^2+4)m_1^2+3\sqrt{m_1^2(9m_2^2+8)}-8m_2m_1+4\right)}{v^2}}}{2\sqrt{2}m_1m_2}\right)$

and $J = \frac{vw_2\sqrt{\frac{m_1^2m_2^2\left(-(9m_2^2+4)m_1^2+3\sqrt{m_1^2(9m_2^2+8)}-8m_2m_1+4\right)}{v^2}}}{2\sqrt{2}m_1m_2}.$

Family 3: the constant values are taken as $d_1 = -d_3$, $d_5 = -id_3$, $v = -\frac{\sqrt{m_1^2(9m_2^2+8)-8}-3m_1m_2}{4d_3}$, $b_1 = -8m_1m_2$ while w_1, w_2, d_2, d_4, d_6, b_2 are the free parameters.

Substituting them in Eq. (12) and then in Eq. (10) the result is, obtained such as

$$\lambda_{1,3}(\eta) = \frac{\frac{G}{d_3}e^{G(d_2-d_3\eta)} + \frac{G}{d_3}Gw_1e^{-G(d_3\eta+d_4)} + \frac{G}{d_3}iGw_2\sin(G(d_6-id_3\eta))}{e^{G(d_2-d_3\eta)} + w_1e^{-G(d_3\eta+d_4)} + w_2\cos(G(d_6-id_3\eta))}. \tag{17}$$

The breather wave solution to Eq. (4) is gained as:

$$\upsilon_{1,3}(x,t) = -\frac{\frac{G}{d_3}\left(-iw_2e^{(-G(d_3(x-m_1t)+d_4))}\sin(G(d_6-id_3(x-m_1t))) + e^{(d_2+d_4)G} + w_1\right)}{4\left(w_2e^{-G(d_3(x-m_1t)+d_4)}\cos(G(d_6-id_3(x-m_1t))) + e^{G(d_2+d_4)} + w_1\right)}, \tag{18}$$

where $G = \frac{\left(3m_1m_2 - \sqrt{m_1^2(9m_2^2+8)-8}\right)}{4d_3}$.

2. Interaction via double exponents: we find double exponents solutions by using the transformation such as[10,36]:

$$f = w_1\exp(d_1\eta + d_2) + w_2\exp(d_3\eta + d_4). \tag{19}$$

By substituting Eq. (19) and its derivatives to the third order into Eq. (9), simplifying and collecting like terms exponential functions with the same powers, and setting each of the resulting expressions to 0, we can determine the values of some of the parameters as follows:

Family 1: the constant values are taken as $d_1 = \frac{1}{2}\left(-\sqrt{m_2^2m_1^2 - 4m_1^2 + 4} - m_1m_2\right)$, $d_3 = 0$, $b_1 = 3\sqrt{m_2^2m_1^2 - 4m_1^2 + 4} + m_1m_2$, $b_2 = 6$, while w_1, w_2, d_2, d_4, are the free parameters.

Substituting them in Eq. (19) and then in Eq. (10) the result is, obtained such as

$$\lambda_{2,1}(\eta) = \frac{\left(-\sqrt{m_2^2m_1^2 - 4m_1^2 + 4} - m_1m_2\right)w_1\exp\left(d_2 + \frac{1}{2}\eta\left(-\sqrt{m_2^2m_1^2 - 4m_1^2 + 4} - m_1m_2\right)\right)}{2\left(w_1\exp\left(d_2 + \frac{1}{2}\eta\left(-\sqrt{m_2^2m_1^2 - 4m_1^2 + 4} - m_1m_2\right)\right) + e^{d_4}w_2\right)}. \tag{20}$$

The interaction of double exponents solution to Eq. (4) is gained as:

$$\upsilon_{2,1}(x,t) = -\frac{\left(\sqrt{(m_2^2-4)m_1^2+4} + m_1m_2\right)w_1\exp\left(d_2 + \frac{1}{2}\left(\sqrt{(m_2^2-4)m_1^2+4} + m_1m_2\right)(m_1^2t-x)\right)}{2\left(w_1\exp\left(d_2 - \frac{1}{2}\left(\sqrt{(m_2^2-4)m_1^2+4} + m_1m_2\right)(x-m_1^2t)\right) + e^{d_4}w_2\right)}. \tag{21}$$

Family 2: the constant values are taken as $d_1 = \frac{1}{2}\left(-\sqrt{(m_1m_2-d_3)^2 - 4(1-m_1^2)} + d_3 - m_1m_2\right)$, $b_1 = \frac{-d_3\sqrt{(m_1m_2-d_3)^2-4(1-m_1^2)}+d_3m_1m_2-d_3^2+2m_1^2-2}{d_3}$, $b_2 = \frac{3\left(d_3\sqrt{(m_1m_2-d_3)^2-4(1-m_1^2)}-d_3m_1m_2+d_3^2\right)}{2d_3^2}$, while w_1, w_2, d_2, d_3, d_4, are the free parameters.

Substituting them in Eq. (19) and then in Eq. (10) the result is, obtained such as

$$\lambda_{2,2}(\eta) = \frac{\frac{1}{2}w_1\left(-\sqrt{(m_1 m_2 - d_3)^2 - 4\left(1 - m_1^2\right)} + d_3 - m_1 m_2\right)e^{\frac{1}{2}\eta\left(-\sqrt{(m_1 m_2 - d_3)^2 - 4\left(1 - m_1^2\right)} + d_3 - m_1 m_2\right) + d_2} + d_3 w_2 e^{d_3\eta + d_4}}{w_1 e^{\frac{1}{2}\eta\left(-\sqrt{(m_1 m_2 - d_3)^2 - 4\left(1 - m_1^2\right)} + d_3 - m_1 m_2\right) + d_2} + w_2 e^{d_3\eta + d_4}}.$$

(22)

The interaction of double exponents solution to Eq. (4) is gained as:

$$\upsilon_{2,2}(x,t) = \frac{d_3 w_2 e^{d_3\left(x - m_1^2 t\right) + d_4} - \frac{1}{2}w_1\left(\sqrt{(d_3 - m_1 m_2)^2 + 4\left(m_1^2 - 1\right)} - d_3 + m_1 m_2\right)e^{d_2 - \frac{1}{2}\left(\sqrt{(d_3 - m_1 m_2)^2 + 4\left(m_1^2 - 1\right)} - d_3 + m_1 m_2\right)\left(x - m_1^2 t\right)}}{w_1 e^{d_2 - \frac{1}{2}\left(\sqrt{(d_3 - m_1 m_2)^2 + 4\left(m_1^2 - 1\right)} - d_3 + m_1 m_2\right)\left(x - m_1^2 t\right)} + w_2 e^{d_3\left(x - m_1^2 t\right) + d_4}}.$$

(23)

3. Lump periodic: we find some solutions using the function[36]

$$f = (d_1\eta + d_2)^2 + (d_3\eta + d_4)^2 + \cos(d_5\eta + d_6) + d_7.$$

(24)

By substituting Eq. (24) and its derivatives to the third order into Eq. (9), simplifying and collecting like terms η, exponential functions, and trigonometric functions with the same powers, and setting each of the resulting expressions to 0, we can determine the values of some of the parameters as follows:

Family 1: the constant values are taken as $d_1 = 0$, $d_3 = 0$, $d_5 = -\frac{\sqrt{1 - m_1^2}}{\sqrt{2}}$, $d_7 = -d_2^2 - d_4^2$, $b_1 = -2m_1 m_2$, $b_2 = 6$, while d_2, d_4, are free parameters.

Substituting them in Eq. (24) and then in Eq. (10) the result is, obtained such as

$$\lambda_{3,1}(\eta) = \frac{\sqrt{1 - m_1^2}}{\sqrt{2}}\tan\left(d_6 - \frac{\eta\sqrt{1 - m_1^2}}{\sqrt{2}}\right).$$

(25)

The Lump wave solution to Eq. (4) is gained as:

$$\upsilon_{3,1}(x,t) = \frac{\sqrt{1 - m_1^2}}{\sqrt{2}}\tan\left(d_6 + \frac{\sqrt{1 - m_1^2}(m_1 t - x)}{\sqrt{2}}\right).$$

(26)

Family 2: the constant values are taken as $d_3 = -\frac{d_1 d_2}{d_4}$, $d_5 = 0$, $d_7 = -d_2^2 - d_4^2$, while d_2, d_4, are free parameters.

Substituting them in Eq. (24) and then in Eq. (10) the result is, obtained such as

$$\lambda_{3,2}(\eta) = \frac{2d_1(d_1\eta + d_2) - \frac{2d_1 d_2\left(d_4 - \frac{d_1 d_2\eta}{d_4}\right)}{d_4}}{(d_1\eta + d_2)^2 + \left(d_4 - \frac{d_1 d_2\eta}{d_4}\right)^2 - d_2^2 - d_4^2 + \cos(d_6)}.$$

(27)

The Lump wave solution to Eq. (4) is gained as:

$$\upsilon_{3,2}(x,t) = \frac{2d_1^2\left(d_2^2 + d_4^2\right)(x - m_1 t)}{d_1^2\left(d_2^2 + d_4^2\right)(x - m_1 t)^2 + d_4^2\cos(d_6)}.$$

(28)

4. Mixed type: we find mixed type solutions by using the transformation such as[10,36]:

$$f = w_1\exp(v(d_1\eta + d_2)) + w_2\exp(-v(d_1\eta + d_2)) + w_3\sin(v(d_3\eta + d_4)) + w_4\sinh(v(d_5\eta + d_6)).$$

(29)

By substituting Eq. (29) and its derivatives to the third order into Eq. (10), simplifying and collecting like terms, exponential functions, trigonometric functions and hyperbolic functions with the same powers, and setting each of the resulting expressions to 0, we can determine the values of some of the parameters as follows:

Family 1: the constant values are taken as $w_1 = 0$, $w_2 = 0$, $d_3 = \frac{\sqrt{1 - m_1^2}}{\sqrt{2}v}$, $d_5 = \frac{\sqrt{m_1^2 - 1}}{\sqrt{2}v}$, $b_1 = -2m_1 m_2$, $b_2 = 6$, while d_4, d_6, w_3, w_4, v, are free parameters.

Substituting them in Eq. (29) and then in Eq. (10) the result is, obtained such as

$$\lambda_{4,1}(\eta) = \frac{\frac{\sqrt{1 - m_1^2}w_3\cos\left(v\left(d_4 + \frac{\eta\sqrt{1 - m_1^2}}{\sqrt{2}v}\right)\right)}{\sqrt{2}} + \frac{\sqrt{m_1^2 - 1}w_4\cosh\left(v\left(d_6 + \frac{\eta\sqrt{m_1^2 - 1}}{\sqrt{2}v}\right)\right)}{\sqrt{2}}}{w_3\sin\left(v\left(d_4 + \frac{\eta\sqrt{1 - m_1^2}}{\sqrt{2}v}\right)\right) + w_4\sinh\left(v\left(d_6 + \frac{\eta\sqrt{m_1^2 - 1}}{\sqrt{2}v}\right)\right)}.$$

(30)

The mixed type solution to Eq. (4) is gained as:

$$v_{4,1}(x,t) = \frac{\sqrt{1-m_1^2}\,w_3\cos\left(d_4v+\frac{1}{2}\sqrt{2-2m_1^2}(x-m_1t)\right)+\sqrt{m_1^2-1}\,w_4\cosh\left(d_6v+\frac{\sqrt{m_1^2-1}(x-m_1t)}{\sqrt{2}}\right)}{\sqrt{2}\left(w_3\sin\left(d_4v+\frac{1}{2}\sqrt{2-2m_1^2}(x-m_1t)\right)+w_4\sinh\left(d_6v+\frac{\sqrt{m_1^2-1}(x-m_1t)}{\sqrt{2}}\right)\right)}.$$

(31)

Family 2: The constant values are taken as $w_1=0$, $d_1=\frac{\sqrt{m_1^2-1}}{\sqrt{2}v}$, $d_3=\frac{\sqrt{1-m_1^2}}{\sqrt{2}v}$, $d_5=\frac{\sqrt{m_1^2-1}}{\sqrt{2}v}$, $b_1=-2m_1m_2$, $b_2=6$, while d_2, d_4, d_6, w_2, w_3, w_4, v, are free parameters.

Substituting them in Eq. (29) and then in Eq. (10) the result is, obtained such as

$$\lambda_{4,2}(\eta)=\frac{-\frac{\sqrt{m_1^2-1}\,w_2 e^{-v\left(d_2+\frac{\eta\sqrt{m_1^2-1}}{\sqrt{2}v}\right)}}{\sqrt{2}}+\frac{\sqrt{1-m_1^2}\,w_3\cos\left(v\left(d_4+\frac{\eta\sqrt{1-m_1^2}}{\sqrt{2}v}\right)\right)}{\sqrt{2}}+\frac{\sqrt{m_1^2-1}\,w_4\cosh\left(v\left(d_6+\frac{\eta\sqrt{m_1^2-1}}{\sqrt{2}v}\right)\right)}{\sqrt{2}}}{w_2 e^{-v\left(d_2+\frac{\eta\sqrt{m_1^2-1}}{\sqrt{2}v}\right)}+w_3\sin\left(v\left(d_4+\frac{\eta\sqrt{1-m_1^2}}{\sqrt{2}v}\right)\right)+w_4\sinh\left(v\left(d_6+\frac{\eta\sqrt{m_1^2-1}}{\sqrt{2}v}\right)\right)}.$$

(32)

The mixed type solution to Eq. (4) is gained as:

$$v_{4,2}(x,t)=\frac{e^{d_2v+\frac{\sqrt{m_1^2-1}(x-m_1t)}{\sqrt{2}}}\left(\sqrt{1-m_1^2}\,w_3\cos(G)+\sqrt{m_1^2-1}\,w_4\cosh(G)\right)-\sqrt{m_1^2-1}\,w_2}{\sqrt{2}\left(e^{d_2v+\frac{\sqrt{m_1^2-1}(x-m_1t)}{\sqrt{2}}}\left(w_3\sin\left(d_4v+\frac{1}{2}\sqrt{2-2m_1^2}(x-m_1t)\right)+w_4\sinh(G)\right)+w_2\right)}.$$

(33)

Where $G=d_6v+\frac{\sqrt{m_1^2-1}(x-m_1t)}{\sqrt{2}}$.

Family 3: The constant values are taken as $w_1=0$, $w_4=0$, $d_3=-\frac{\sqrt{1-m_1^2}}{\sqrt{2}v}$, $b_1=-2m_1m_2$, $b_2=\frac{3(2d_1^2v^2+m_1^2-1)}{2d_1^2v^2}$, while d_1, d_4, d_5, d_6, w_2, w_3, v, are free parameters.

Substituting them in Eq. (29) and then in Eq. (10) the result is, obtained such as

$$\lambda_{4,3}(\eta)=\frac{d_1vw_2\left(-e^{-v(d_1\eta+d_2)}\right)-\frac{\sqrt{1-m_1^2}\,w_3\cos\left(v\left(d_4-\frac{\eta\sqrt{1-m_1^2}}{\sqrt{2}v}\right)\right)}{\sqrt{2}}}{w_3\sin\left(v\left(d_4-\frac{\eta\sqrt{1-m_1^2}}{\sqrt{2}v}\right)\right)+w_2e^{-v(d_1\eta+d_2)}}.$$

(34)

The mixed type solution to Eq. (4) is gained as:

$$v_{4,3}(x,t)=-\frac{\sqrt{2-2m_1^2}\,w_3e^{v(d_1(x-m_1t)+d_2)}\cos\left(d_4v+\frac{1}{2}\sqrt{2-2m_1^2}(m_1t-x)\right)+2d_1vw_2}{2\left(w_3e^{v(d_1(x-m_1t)+d_2)}\sin\left(d_4v+\frac{1}{2}\sqrt{2-2m_1^2}(m_1t-x)\right)+w_2\right)}.$$

(35)

Family 4: the constant values are taken as $w_2=0$, $w_4=0$, $v=\frac{\sqrt{1-m_1^2}}{\sqrt{2}d_3}$, $b_1=-2m_1m_2$, while d_1, d_2, d_4, w_2, w_3, v, are free parameters.

Substituting them in Eq. (29) and then in Eq. (10) the result is, obtained such as

$$\lambda_{4,4}(\eta)=\frac{\frac{d_1\sqrt{1-m_1^2}\,w_1e^{\frac{\sqrt{1-m_1^2}(d_1\eta+d_2)}{\sqrt{2}d_3}}}{\sqrt{2}d_3}+\frac{\sqrt{1-m_1^2}\,w_3\cos\left(\frac{\sqrt{1-m_1^2}(d_3\eta+d_4)}{\sqrt{2}d_3}\right)}{\sqrt{2}}}{w_1e^{\frac{\sqrt{1-m_1^2}(d_1\eta+d_2)}{\sqrt{2}d_3}}+w_3\sin\left(\frac{\sqrt{1-m_1^2}(d_3\eta+d_4)}{\sqrt{2}d_3}\right)}.$$

(36)

The mixed type solution to Eq. (4) is gained as:

$$v_{4,4}(x,t)=\frac{\sqrt{1-m_1^2}\left(d_1w_1\exp\left(\frac{\sqrt{1-m_1^2}(d_1(x-m_1t)+d_2)}{\sqrt{2}d_3}\right)+d_3w_3\cos\left(\frac{\sqrt{1-m_1^2}(d_3(x-m_1t)+d_4)}{\sqrt{2}d_3}\right)\right)}{\sqrt{2}d_3\left(w_1\exp\left(\frac{\sqrt{1-m_1^2}(d_1(x-m_1t)+d_2)}{\sqrt{2}d_3}\right)+w_3\sin\left(\frac{\sqrt{1-m_1^2}(d_3(x-m_1t)+d_4)}{\sqrt{2}d_3}\right)\right)}.$$

(37)

5. Multiwave: we find multiwave solutions by using the transformation such as[10,36]:

$$f=w_2\cos(d_3\eta+d_4)+w_1\cosh(d_1\eta+d_2)+w_3\cosh(d_5\eta+d_6).$$

(38)

By substituting Eq. (38) and its derivatives to the third order into Eq. (9), simplifying and collecting like terms of trigonometric functions and hyperbolic functions with the same powers, and setting each of the resulting expressions to 0, we can determine the values of some of the parameters as follows:

Family 1: the constant values are taken as $w_3 = 0$, $d_1 = \frac{\sqrt{m_1^2 - 1}}{\sqrt{2}}$, $d_3 = \frac{\sqrt{1 - m_1^2}}{\sqrt{2}}$, while d_2, d_4, w_1, w_2, are free parameters.

Substituting them in Eq. (38) and then in Eq. (10) the result is, obtained such as

$$\lambda_{5,1}(\eta) = \frac{\frac{\sqrt{m_1^2 - 1}w_1 \sinh\left(d_2 + \frac{\eta\sqrt{m_1^2 - 1}}{\sqrt{2}}\right)}{\sqrt{2}} - \frac{\sqrt{1 - m_1^2}w_2 \sin\left(d_4 + \frac{\eta\sqrt{1 - m_1^2}}{\sqrt{2}}\right)}{\sqrt{2}}}{w_2 \cos\left(d_4 + \frac{\eta\sqrt{1 - m_1^2}}{\sqrt{2}}\right) + w_1 \cosh\left(d_2 + \frac{\eta\sqrt{m_1^2 - 1}}{\sqrt{2}}\right)}. \tag{39}$$

The multiwave solution to Eq. (4) is gained as:

$$\upsilon_{5,1}(x,t) = \frac{\sqrt{m_1^2 - 1}w_1 \sinh\left(d_2 + \frac{\sqrt{m_1^2 - 1}(x - m_1 t)}{\sqrt{2}}\right) - \sqrt{1 - m_1^2}w_2 \sin\left(d_4 + \frac{\sqrt{1 - m_1^2}(x - m_1 t)}{\sqrt{2}}\right)}{\sqrt{2}\left(w_2 \cos\left(d_4 + \frac{\sqrt{1 - m_1^2}(x - m_1 t)}{\sqrt{2}}\right) + w_1 \cosh\left(d_2 + \frac{\sqrt{m_1^2 - 1}(x - m_1 t)}{\sqrt{2}}\right)\right)}. \tag{40}$$

Family 2: the constant values are taken as $w_3 = 0$, $d_1 = 0$, $d_3 = -\frac{\sqrt{1 - m_1^2}}{\sqrt{2}}$, while d_2, d_4, w_1, w_2, are free parameters.

Substituting them in Eq. (38) and then in Eq. (10) the result is, obtained such as

$$\lambda_{5,2}(\eta) = \frac{\sqrt{1 - m_1^2}w_2 \sin\left(d_4 - \frac{\eta\sqrt{1 - m_1^2}}{\sqrt{2}}\right)}{\sqrt{2}\left(w_2 \cos\left(d_4 - \frac{\eta\sqrt{1 - m_1^2}}{\sqrt{2}}\right) + w_1 \cosh(d_2)\right)}. \tag{41}$$

The multiwave solution to Eq. (4) is gained as:

$$\upsilon_{5,2}(x,t) = \frac{\sqrt{1 - m_1^2}w_2 \sin\left(d_4 - \frac{\sqrt{1 - m_1^2}(x - m_1 t)}{\sqrt{2}}\right)}{\sqrt{2}\left(w_2 \cos\left(d_4 - \frac{\sqrt{1 - m_1^2}(x - m_1 t)}{\sqrt{2}}\right) + w_1 \cosh(d_2)\right)}. \tag{42}$$

Family 3: the constant values are taken as $w_2 = 0$, $w_3 = 0$, $d_1 = \frac{\sqrt{m_1^2 - 1}}{\sqrt{2}}$, while d_2, d_4, w_1, are free parameters.

Substituting them in Eq. (38) and then in Eq. (10) the result is, obtained such as

$$\lambda_{5,3}(\eta) = \frac{\sqrt{m_1^2 - 1}}{\sqrt{2}} \tanh\left(d_2 + \frac{\eta\sqrt{m_1^2 - 1}}{\sqrt{2}}\right). \tag{43}$$

The multiwave solution to Eq. (4) is gained as:

$$\upsilon_{5,3}(x,t) = \frac{\sqrt{m_1^2 - 1}}{\sqrt{2}} \tanh\left(d_2 + \frac{\sqrt{m_1^2 - 1}(x - m_1 t)}{\sqrt{2}}\right). \tag{44}$$

Family 4: the constant values are taken as $w_1 = 0$, $w_3 = 0$, $d_3 = -\frac{\sqrt{1 - m_1^2}}{\sqrt{2}}$, while d_4, w_2, are free parameters.

Substituting them in Eq. (38) and then in Eq. (10) the result is, obtained such as

$$\lambda_{5,4}(\eta) = \frac{\sqrt{1 - m_1^2}}{\sqrt{2}} \tan\left(d_4 - \frac{\eta\sqrt{1 - m_1^2}}{\sqrt{2}}\right). \tag{45}$$

The multiwave solution to Eq. (4) is gained as:

$$\upsilon_{5,4}(x,t) = \frac{\sqrt{1 - m_1^2}}{\sqrt{2}} \tan\left(d_4 - \frac{\sqrt{1 - m_1^2}(x - m_1 t)}{\sqrt{2}}\right). \tag{46}$$

6. Periodic cross kink: we find periodic cross kink solutions by using the transformation such as[10,36]:

$$f = \exp\left(-v(d_1\eta + d_2)\right) + w_1 \exp\left(v(d_3\eta + d_4)\right) + w_2 \cos\left(v(d_5\eta + d_6)\right) + w_3 \cosh\left(v(d_7\eta + d_8)\right) + d_9. \tag{47}$$

By substituting Eq. (47) and its derivatives to the third order into Eq. (9), simplifying and collecting like terms of exponential functions, trigonometric functions and hyperbolic functions with the same powers, and setting each of the resulting expressions to 0, we can determine the values of some of the parameters as follows:

Family 1: the constant values are taken as $w_2 = 0$, $d_1 = -d_3$, $d_7 = \frac{\sqrt{\frac{1}{3}d_3 v((b_2-9)d_3 v + 6m_1 m_2) + m_1^2 - 1}}{v}$, $d_9 = 0$, $b_1 = -\frac{2(b_2 d_3^2 v^2 - 3m_1^2 + 3)}{3d_3 v}$, while d_2, d_4, d_6, w_1, w_3, v are free parameters.

Substituting them in Eq. (47) and then in Eq. (10) the result is, obtained such as

$$\lambda_{6,1}(\eta) = \frac{-\frac{v(G)}{4(b_2 v^2 + 2v^2)}e^{-v\left(\frac{\eta(G)}{4(b_2 v^2 + 2v^2)} + d_2\right)} - \frac{1}{2}\sqrt{m_1^2 - 1}\, w_2 \sin\left(v\left(d_6 + \frac{\eta\sqrt{m_1^2-1}}{2v}\right)\right)}{e^{-v\left(\frac{\eta(G)}{4(b_2 v^2 + 2v^2)} + d_2\right)} + w_2 \cos\left(v\left(d_6 + \frac{\eta\sqrt{m_1^2-1}}{2v}\right)\right) + w_3 \cosh(d_8 v)}. \tag{48}$$

where $G = \sqrt{(-4b_1 v - 9m_1 m_2 v)^2 - 4(m_1^2 - 1)(2b_2 v^2 + 4v^2)} + 4b_1 v + 9m_1 m_2 v$.

The periodic cross kink solution to Eq. (4) is gained as:

$$\upsilon_{6,1}(x,t) = \frac{\sqrt{3}w_3 J e^{v(d_3(m_1 t - x) + d_2)} \sinh\left((x-m_1 t)J + d_8 v\right) + 3d_3 v\left(w_1 e^{(d_2+d_4)v} + 1\right)}{3\left(w_3 e^{v(d_3(m_1 t - x) + d_2)} \cosh\left((x-m_1 t)J + d_8 v\right) + w_1 e^{(d_2+d_4)v} + 1\right)}, \tag{49}$$

where $J = \sqrt{(b_2-9)d_3^2 v^2 + 6d_3 m_1 m_2 v + 3(m_1^2 - 1)}$.

Family 2: the constant values are taken as $w_1 = 0$, $w_2 = 0$, $d_7 = -\frac{\sqrt{3d_1^2 v^2 - 2m_1^2 + 2}}{\sqrt{2}v}$, $b_1 = -2m_1 m_2$, $b_2 = 6$, while d_1, d_2, d_8, d_9, w_3, v are free parameters.

Substituting them in Eq. (47) and then in Eq. (10) the result is, obtained such as

$$\lambda_{6,2}(\eta) = \frac{d_1 v\left(-e^{-v(d_1\eta + d_2)}\right) - \frac{w_3 \sqrt{3d_1^2 v^2 - 2m_1^2 + 2}\, \sinh\left(v\left(d_8 - \frac{\eta\sqrt{3d_1^2 v^2 - 2m_1^2 + 2}}{\sqrt{2}v}\right)\right)}{\sqrt{2}}}{w_3 \cosh\left(v\left(d_8 - \frac{\eta\sqrt{3d_1^2 v^2 - 2m_1^2 + 2}}{\sqrt{2}v}\right)\right) + e^{-v(d_1\eta + d_2)} + d_9}. \tag{50}$$

The periodic cross kink solution to Eq. (4) is gained as:

$$\upsilon_{6,2}(x,t) = -\frac{w_3 \sqrt{6d_1^2 v^2 - 4m_1^2 + 4}\, e^{v(d_1(x-m_1 t) + d_2)} \sinh\left(\sqrt{\frac{3}{2}d_1^2 v^2 - m_1^2 + 1}(m_1 t - x) + d_8 v\right) + 2d_1 v}{2\left(w_3 e^{v(d_1(x-m_1 t) + d_2)} \cosh\left(\sqrt{\frac{3}{2}d_1^2 v^2 - m_1^2 + 1}(m_1 t - x) + d_8 v\right) + d_9 e^{v(d_1(x-m_1 t) + d_2)} + 1\right)}. \tag{51}$$

Family 3: the constant values are taken as $w_1 = 0$, $d_5 = \frac{\sqrt{1-m_1^2}}{\sqrt{2}v}$, $d_7 = \frac{\sqrt{1-m_1^2}}{2v}$, $d_9 = 0$, $b_1 = -2m_1 m_2$, $b_2 = 6$, while d_1, d_2, d_6, d_8, w_2, w_3, v are free parameters.

Substituting them in Eq. (47) and then in Eq. (10) the result is, obtained such as

$$\lambda_{6,3}(\eta) = \frac{-\frac{\sqrt{1-m_1^2}\, w_2 \sin\left(v\left(d_6 + \frac{\eta\sqrt{1-m_1^2}}{\sqrt{2}v}\right)\right)}{\sqrt{2}} + \frac{1}{2}\sqrt{1-m_1^2}\, w_3 \sinh\left(v\left(d_8 + \frac{\eta\sqrt{1-m_1^2}}{2v}\right)\right) + d_1 v\left(-e^{-v(d_1\eta + d_2)}\right)}{w_2 \cos\left(v\left(d_6 + \frac{\eta\sqrt{1-m_1^2}}{\sqrt{2}v}\right)\right) + w_3 \cosh\left(v\left(d_8 + \frac{\eta\sqrt{1-m_1^2}}{2v}\right)\right) + e^{-v(d_1\eta + d_2)}}. \tag{52}$$

The periodic cross kink solution to Eq. (4) is gained as:

$$\upsilon_{6,3}(x,t) = \frac{\sqrt{1-m_1^2}\, e^{v(d_1(x-m_1 t) + d_2)}\left(w_3 \sinh\left(d_8 v + \frac{1}{2}\sqrt{1-m_1^2}(x-m_1 t)\right) - \sqrt{2}w_2 \sin\left(d_6 v + \frac{1}{2}\sqrt{2-2m_1^2}(x-m_1 t)\right)\right) - 2d_1 v}{2\left(w_2 e^{v(d_1(x-m_1 t) + d_2)} \cos\left(d_6 v + \frac{1}{2}\sqrt{2-2m_1^2}(x-m_1 t)\right) + w_3 e^{v(d_1(x-m_1 t) + d_2)} \cosh\left(d_8 v + \frac{1}{2}\sqrt{1-m_1^2}(x-m_1 t)\right) + 1\right)}. \tag{53}$$

Graphical presentations

In this section, we look at the graphical representations of the solutions we've found. The wave shapes depicted below are graphical representations of these solutions. We thoroughly investigate the behavior and distinguishing aspects of the solutions produced from the Heimburg equations through detailed explanations and accompanying

graphs. These studies demonstrate the system's amazing variety of waveforms, emphasizing its potential uses in biomembranes and nerves. Understanding the transmission of electrical impulses and the dynamics of bio-membrane structures in the context of the Heimburg model for biomembranes and nerves requires an understanding of breather waves, lump solitons, mixed multiwave solutions and other interactions. These are nonlinear wave solutions that are localised and oscillate amplitude and width on a periodic basis without changing their general shape. The interaction of dispersion and nonlinearity in the membrane, which influences the passage of electrical signals across nerve fibres, might result in these waves. Their physical importance comes from our understanding of how energy moves through biological membranes and is modulated, which affects the communication and propagation of nerve signals. These solitons may be associated with certain membrane fluctuations or structures,
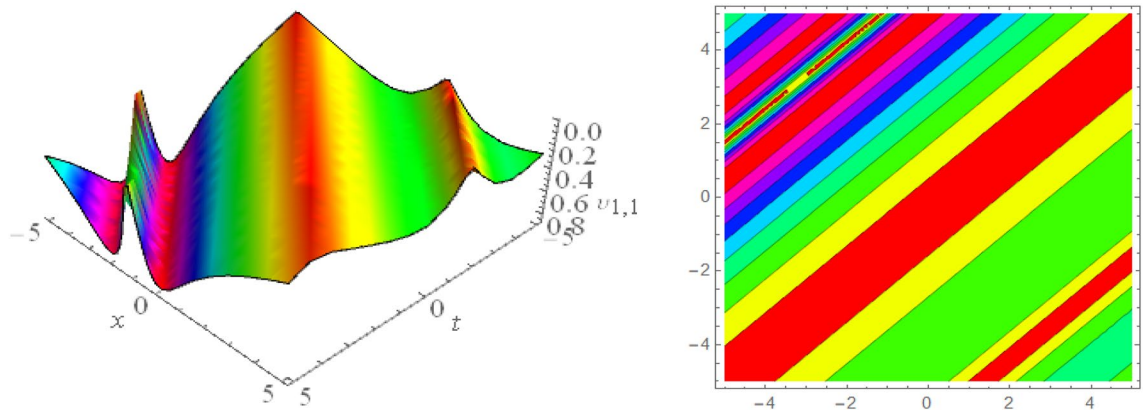
Figure 1. 3D and corresponding contour for solution $\upsilon_{1,1}(x,t)$ with $d_2 = 1.1$, $d_3 = 0.5$, $d_4 = 0.3$, $d_6 = 2.3$, $m_1 = 1.1$, $m_2 = 0.06$, $m_4 = -1.9$, $w_1 = 0.2$, $w_2 = 0.8$.
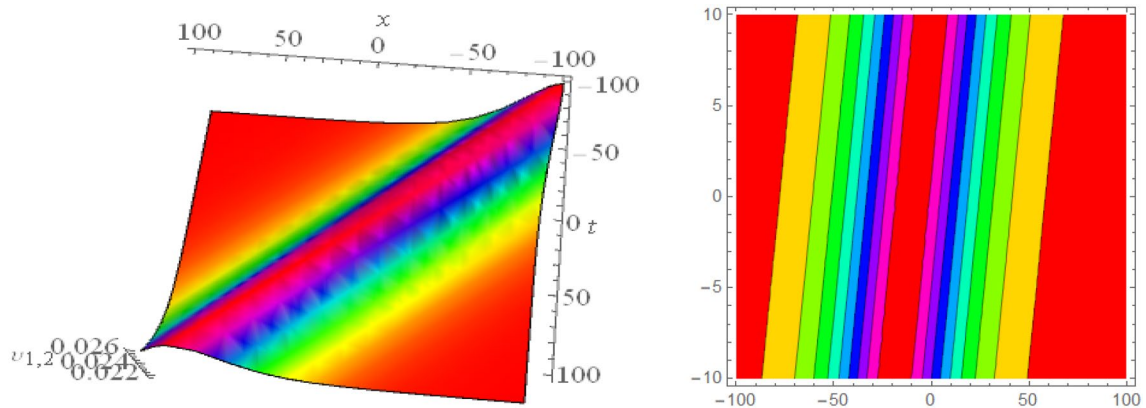
Figure 2. 3D and corresponding contour for solution $\upsilon_{1,2}(x,t)$ with $d_2 = 0.01$, $d_3 = 1.5$, $d_4 = 2.3$, $d_6 = 10.3$, $m_1 = 0.92$, $m_2 = 2.6$, $m_4 = 1$, $v = 0.5$, $w_1 = 0.2$, $w_2 = 2.5$.
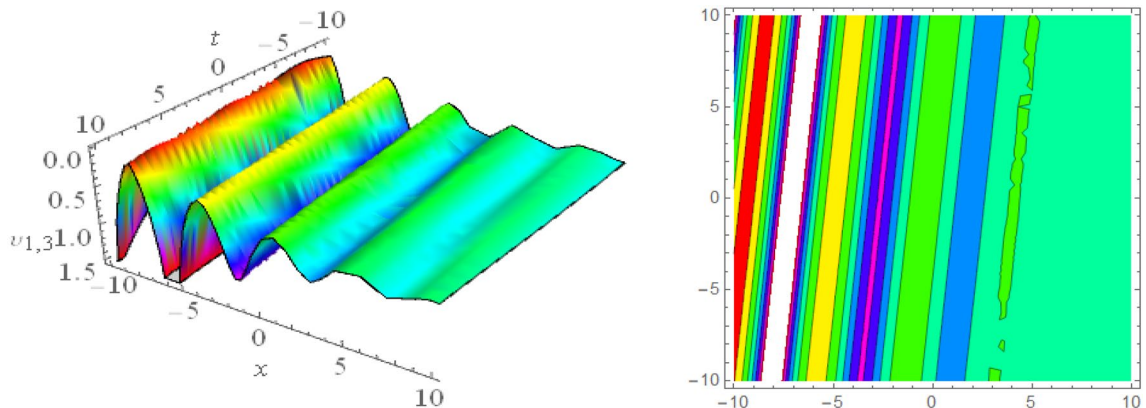
Figure 3. 3D and corresponding contour for solution $\upsilon_{1,3}(x,t)$ with $d_2 = 0.1$, $d_4 = 1$, $d_3 = 1.01$, $d_6 = 0.3$, $m_1 = 0.1$, $m_2 = 1.1$, $m_4 = 1.6$, $v = 0.5$, $w_1 = 10.2$, $w_2 = 6.5$.
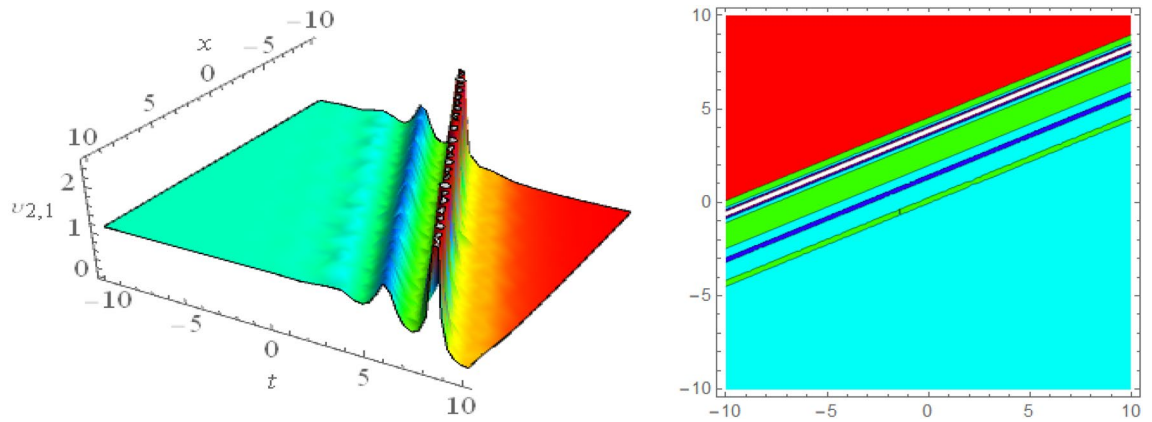
Figure 4. 3D and corresponding contour for solution $v_{2,1}(x,t)$ with $d_2 = 3.1$, $d_4 = 1.1$, $m_1 = -1.5$, $m_2 = 0.36$, $w_1 = 3.5$, $w_2 = 3.2$.
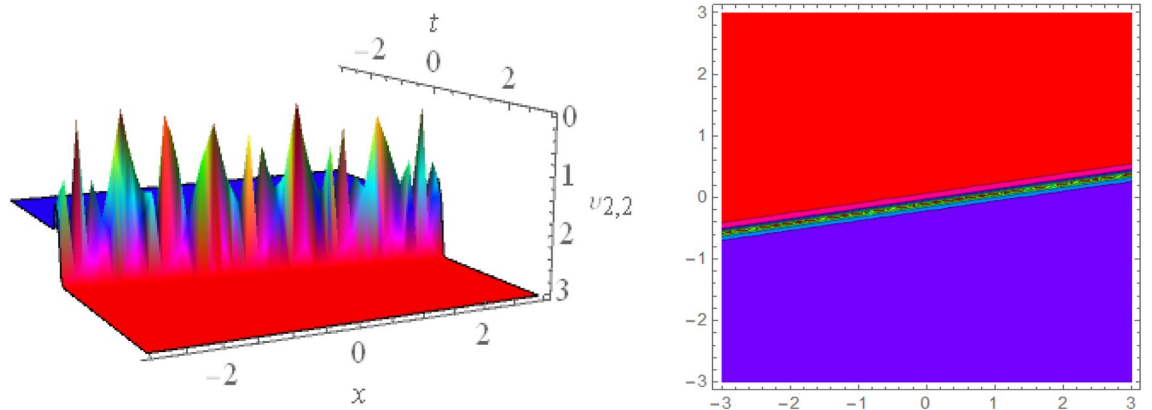
Figure 5. 3D and corresponding contour for solution $v_{2,2}(x,t)$ with $d_2 = 2.1$, $d_3 = 2.1$, $d_4 = 0.1$, $m_1 = 2.5$, $m_2 = 1.36$, $w_1 = 0.5$, $w_2 = 0.2$.
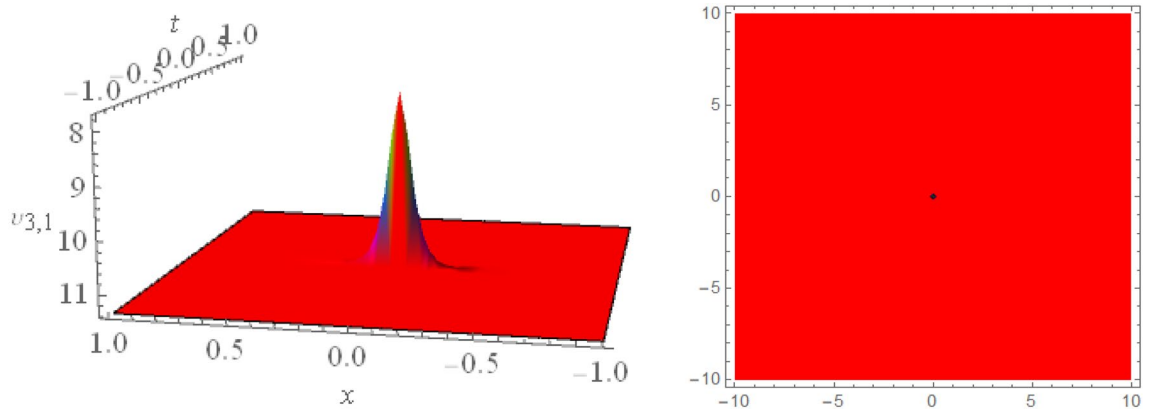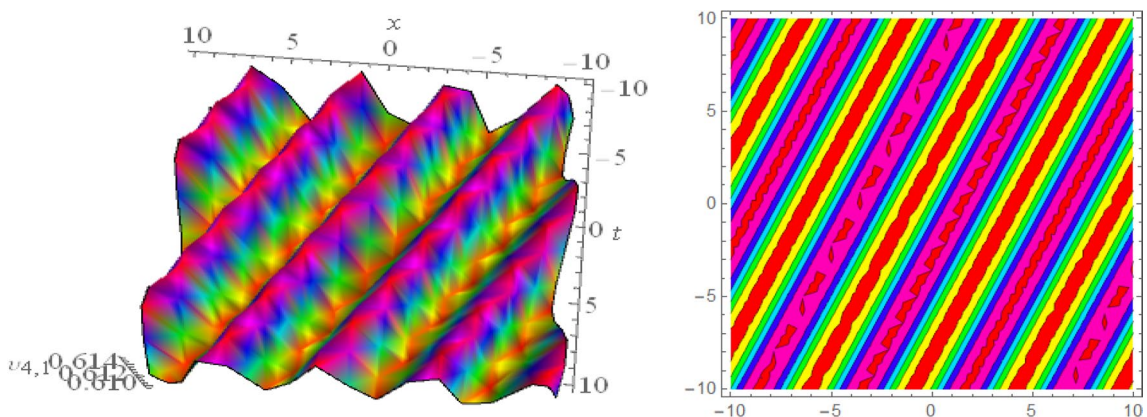

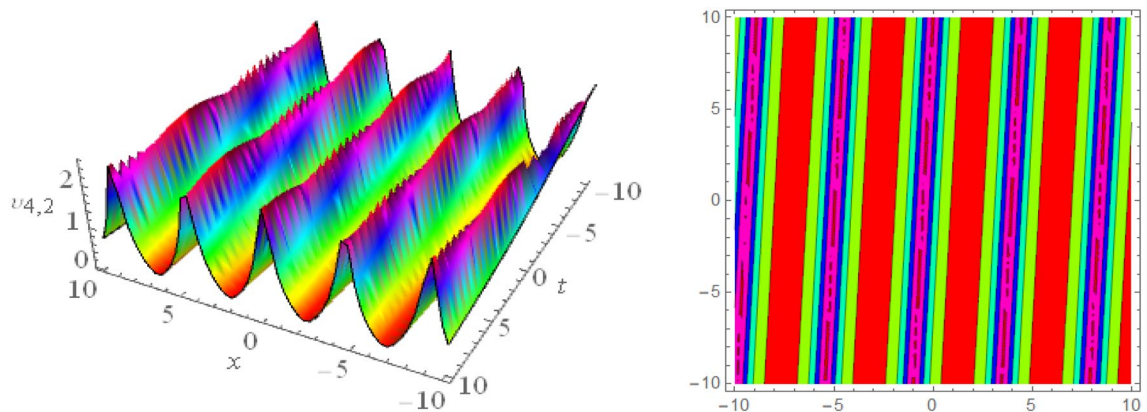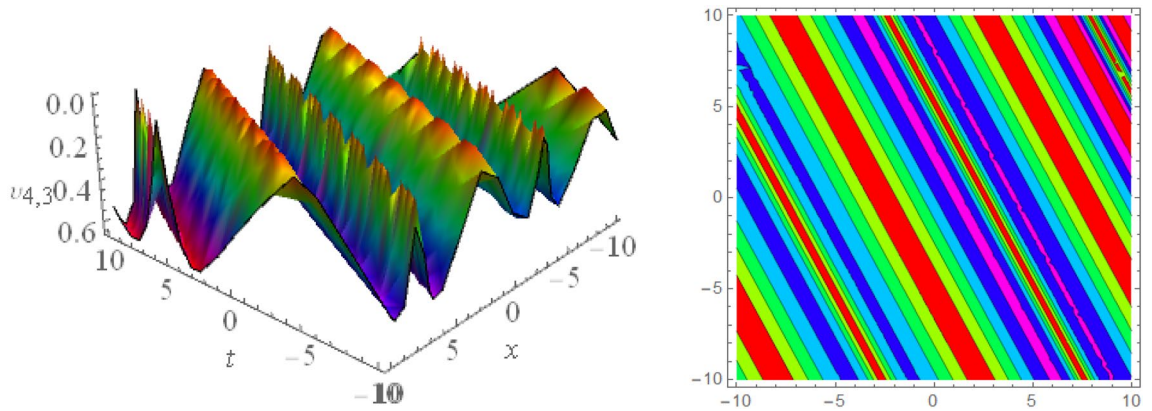**Figure 6.** 3D and corresponding contour for solution $v_{3,1}(x,t)$ with $d_6 = 0.6$, $m_1 = 16.1$.

contributing to both signal transmission and membrane structural integrity. The importance is in comprehending how these localised structures remain stable and persistent in the intricate dynamics of biomembranes and neurons. The Figs. 1, 2, and 3 are drawn for the breather waves while Fig. 4 are the interaction of double exponents. The Figs. 5 and 6 clearly show the lump wave solutions. The Figs. 7, 8 and 9 give us the solitary waves by the mixed type solutions. Figure 10 also shows the limps in their interaction, while Figs. 11 and 12 explore the multiwaves. Figure 13 provided us with the dark soliton while Fig. 14 bright soliton. The Figs. 15, 16, 17 and 18 give us the periodic cross solution in their behaviors. These solutions are very attractive and helpful for the dynamic study of the Heimburg model and their interaction in medicine and the biological sciences.
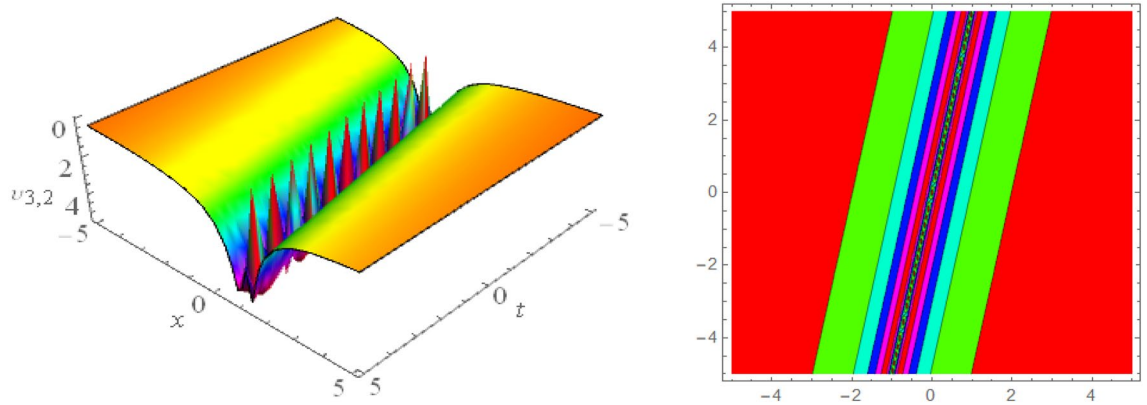
Figure 7. 3D and corresponding contour for solution $v_{3,2}(x, t)$ with $d_1 = 2.5$, $d_2 = 2.5$, $d_4 = 1.5$, $d_6 = 0.6$, $d_7 = 1.7$, $m_1 = 0.2$.

Figure 8. 3D and corresponding contour for solution $v_{4,1}(x, t)$ with $d_4 = 6.1$, $d_6 = 4.1$, $m_1 = 0.5$, $v = 1.5$, $w_3 = 1.6$, $w_4 = 1.5$.
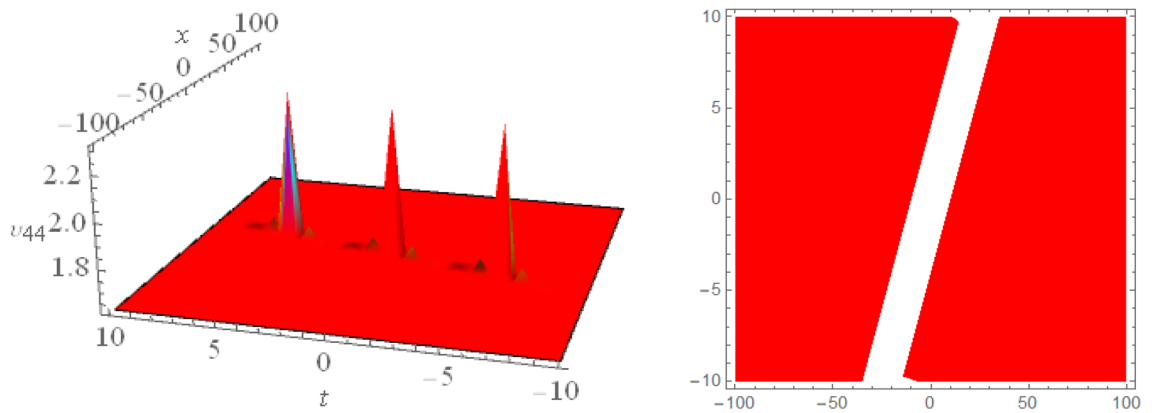

Figure 9. 3D and corresponding contour for solution $v_{4,2}(x, t)$ with $d_2 = 2.1$, $d_4 = 0.1$, $d_6 = 0.1$, $m_1 = 0.05$, $v = 0.25$, $w_2 = 1.03$, $w_3 = 1.08$, $w_4 = 1.6$.

Conclusion

This study, used the Hirota Bilinear technique to explain soliton formation and propagation in biomembranes and nerves offers vital insights into the complex process of nerve impulse generation and transmission. This approach effectively found the exact travelling wave solutions to the Heimburg model of neurology, revealing innovative and different features such as kink, homoclinic wave, lump, mixed wave, multi wave and periodic-wave solutions. The significance of these results cannot be underestimated, because they offer insight into one of the most exciting issues in current biophysics-the basic mechanism that underpins life itself, the nerve impulse. This study has enhanced not just neurophysiology, but also mathematical physics as well. Furthermore, the graphical

12

Figure 10. 3D and corresponding contour for solution $v_{4,3}(x,t)$ with $d_1 = 4.1$, $d_2 = 0.5$, $d_4 = 0.5$, $v = 0.003$, $w_2 = 1.6$, $w_3 = 0.99$.
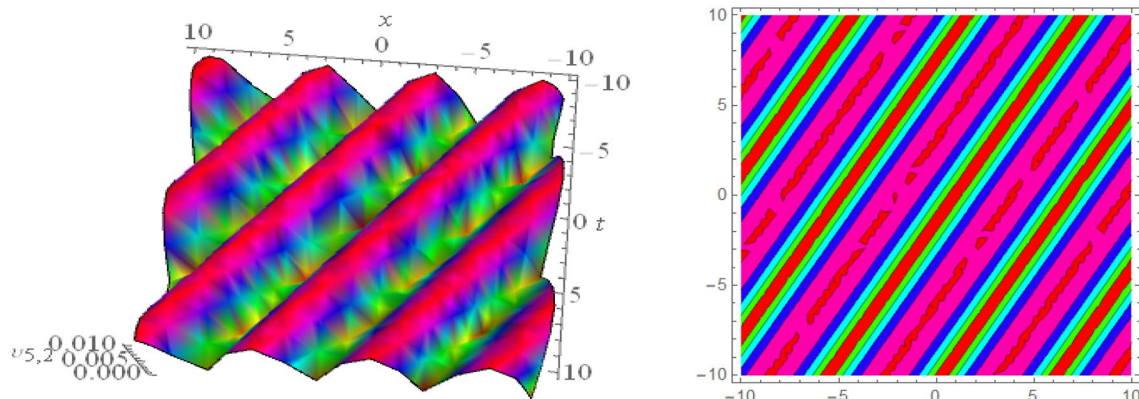

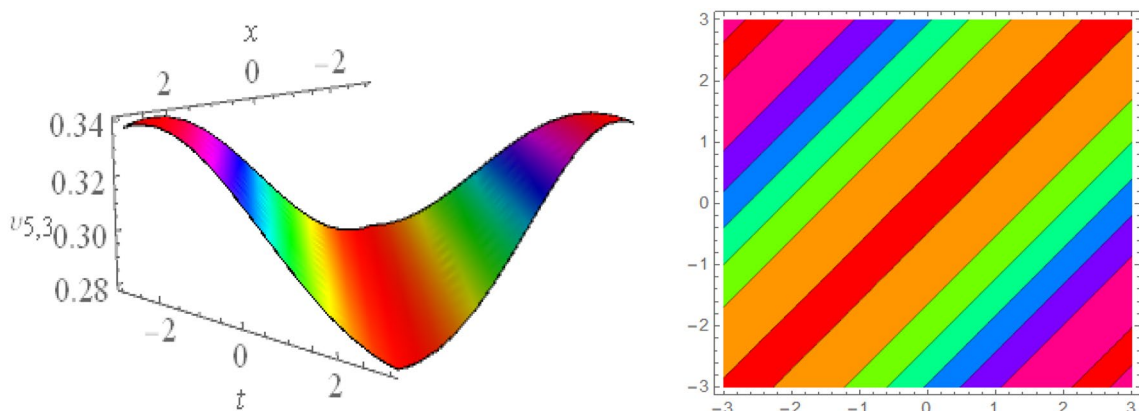**Figure 11.** 3D and corresponding contour for solution $v_{4,4}(x,t)$ with $d_4 = 4.1$, $m_1 = 2.5$.
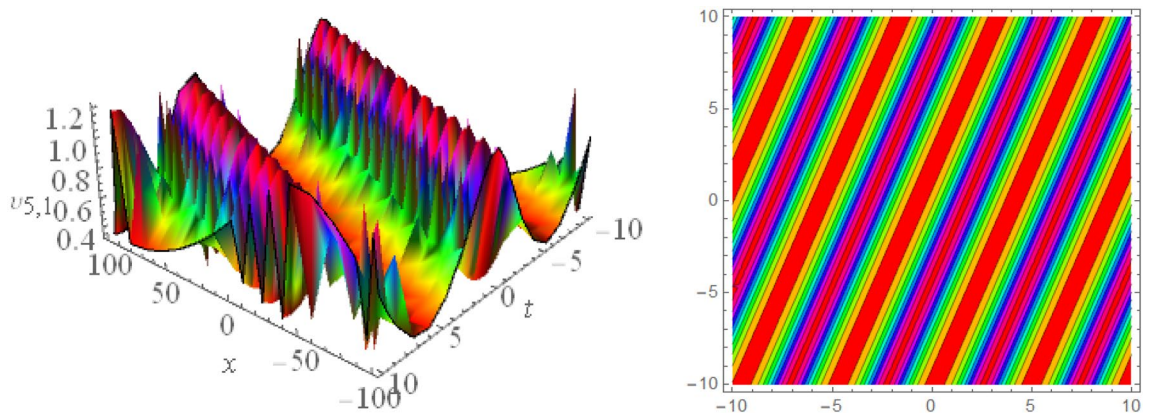
Figure 12. 3D and corresponding contour for solution $v_{5,1}(x,t)$ with $d_2 = 1.01$, $d_4 = 1.05$, $m_1 = 0.4$, $w_1 = 6.1$, $w_2 = 4.5$.

representations of the travelling wave solutions suggest the obtained unique profiles modulate into pulse patterns as they propagate through the axon. This dynamic behaviour gives crucial information for precisely understanding and managing the nerve impulse magnitude. The solutions obtained in this study are very remarkable because they have not being found in previous studies. The use of Mathematica 11.1 to validate these facts strengthens their accuracy and dependability. In the future, these analytic representations of solitary solutions offer possibilities for prospective applications in medicine and biosciences. They could be a useful tool for precise regulation of pulse magnitudes in nerve conduction, allowing for more investigation and breakthroughs in the understanding and treatment of many neurological disorders. Wave propagation issues in biomembranes and neurons, on the

Figure 13. 3D and corresponding contour for solution $v_{5,2}(x,t)$ with $d_2 = 4.1$, $d_4 = 0.5$, $m_1 = 0.65$, $w_1 = 0.51$, $w_2 = 0.29$.
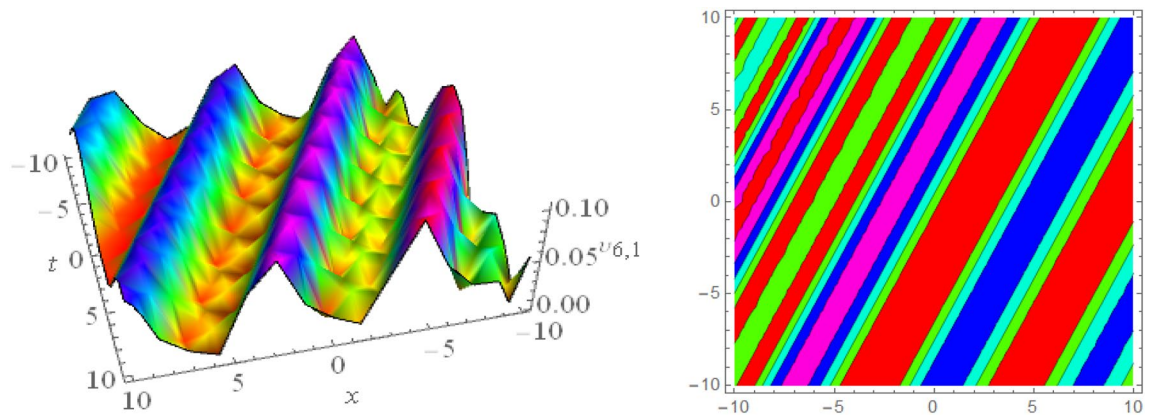

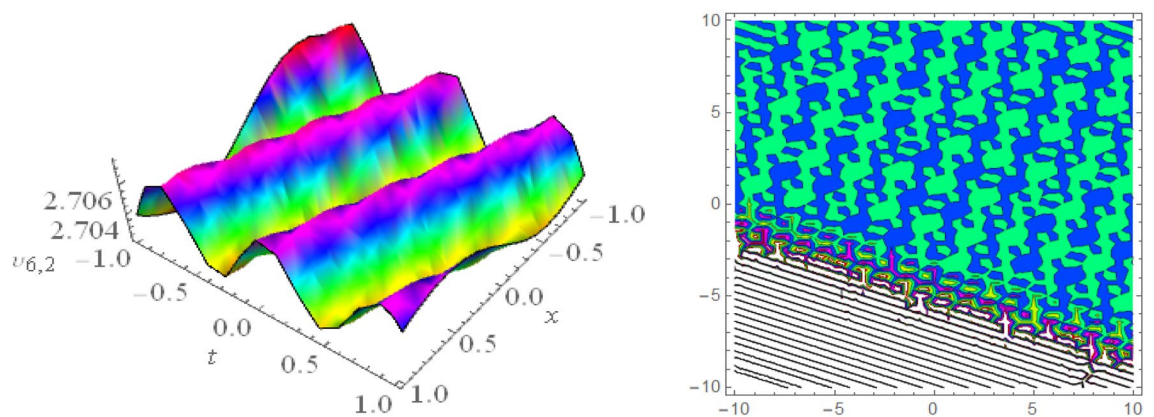**Figure 14.** 3D and corresponding contour for solution $v_{5,3}(x,t)$ with $d_4 = 0.5$, $m_1 = 0.855$.
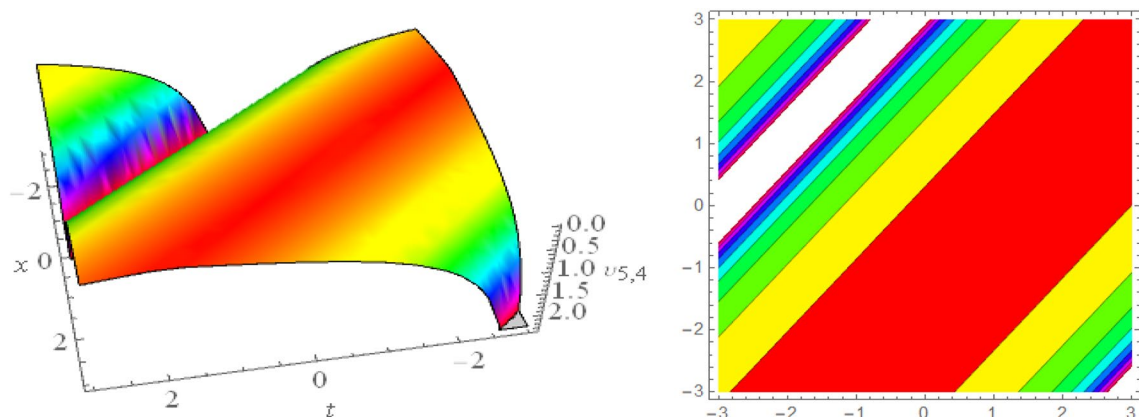
Figure 15. 3D and corresponding contour for solution $v_{5,4}(x,t)$ with $d_2 = 1.5$, $m_1 = 0.9$.

other hand, remain fascinating and challenging. More research is needed to expand on the foundation established by this study and other similar studies, and move further into the complexities surrounding this phenomena. In conclusion, the use of the Hirota Bilinear Method has made a substantial contribution to understanding the complexities of soliton formation and propagation in biomembranes and neurons. The findings of this study provide hope for both fundamental scientific understanding and future practical applications in the realms of medicine and bioscience. As we seek to investigate the intriguing issues of wave propagation in biomembranes, we go on an investigation to gain a better understanding of life's fundamental processes. For the future work this study is helpful to obtained the different types of soliton solutions for the NLPDEs while the bilinear residual network method[14–18] is also powerful technique to obtained the exact solutions for the integrable differential equations.

Figure 16. 3D and corresponding contour for solution $v_{6,1}(x,t)$ with $b_2 = 1.2$, $d_2 = 0.1$, $d_3 = 0.067$, $d_4 = 2.1$, $d_8 = 0.1$, $m_1 = 0.5$, $m_2 = 0.6$, $v = 0.5$, $w_3 = 0.4$, $w_1 = 1.98$.

Figure 17. 3D and corresponding contour for solution $v_{6,2}(x,t)$ with $d_1 = 0.1$, $d_2 = 0.62$, $d_8 = 2.3$, $d_9 = 0.9$, $m_1 = -2.9$, $v = 2.5$, $w_3 = 8.6$.
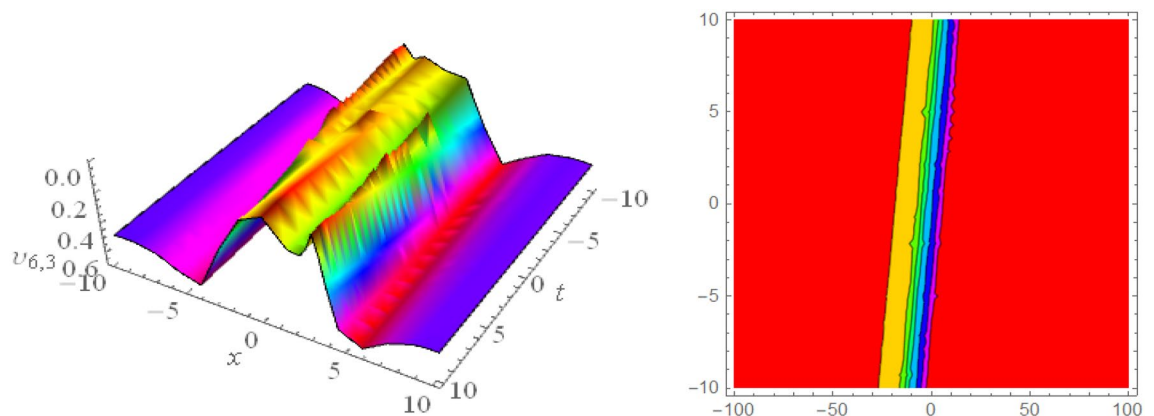
Figure 18. 3D and corresponding contour for solution $v_{6,3}(x,t)$ with $d_1 = 0.1$, $d_2 = 0.62$, $d_6 = 0.03$, $d_8 = 0.02$, $m_1 = 0.05$, $v = 4.5$, $w_2 = 0.6$, $w_3 = 0.5$.

Ethical approval

All the authors demonstrating that they have adhered to the accepted ethical standards of a genuine research study.

Consent to participate

Being the corresponding author, I have consent to participate of all the authors in this research work.

Data availability
Data will be provided on request to the corresponding author.

References
1. Rani, A. *et al.* Application of the $Exp(-\varphi(\xi))$—Expansion method to find the soliton solutions in biomembranes and nerves. *Mathematics* **10**(18), 3372 (2022).
2. Miah, M. M., Seadawy, A. R., Ali, H. S. & Akbar, M. A. Abundant closed form wave solutions to some nonlinear evolution equations in mathematical physics. *J. Ocean Eng. Sci.* **5**(3), 269–278 (2020).
3. Appali, R., Van Rienen, U., & Heimburg, T. A comparison of the Hodgkin–Huxley model and the soliton theory for the action potential in nerves. In *Advances in Planar Lipid Bilayers and Liposomes*. Vol. 16. 275–299. (Academic Press, 2012).
4. Achu, G. F., Tchouobiap, S. M., Kakmeni, F. M. & Tchawoua, C. Periodic soliton trains and informational code structures in an improved soliton model for biomembranes and nerves. *Phys. Rev. E* **98**(2), 022216 (2018).
5. Jian-Rong, Y. & Jie-Jian, M. Soliton solutions of coupled KdV system from Hirota's bilinear direct method. *Commun. Theor. Phys.* **49**(1), 22 (2008).
6. Hereman, W. & Nuseir, A. Symbolic methods to construct exact solutions of nonlinear partial differential equations. *Math. Comput. Simul.* **43**(1), 13–27 (1997).
7. Kivshar, Y. S. & Malomed, B. A. Dynamics of solitons in nearly integrable systems. *Rev. Mod. Phys.* **61**(4), 763 (1989).
8. Arshad, M., Seadawy, A. R., Lu, D. & Jun, W. Modulation instability analysis of modify unstable nonlinear Schrodinger dynamical equation and its optical soliton solutions. *Results Phys.* **7**, 4153–4161 (2017).
9. Yokus, A. & Isah, M. A. Stability analysis and solutions of (2+ 1)-Kadomtsev–Petviashvili equation by homoclinic technique based on Hirota bilinear form. *Nonlinear Dyn.* **109**(4), 3029–3040 (2022).
10. Younas, U., Ren, J., Baber, M. Z., Yasin, M. W., & Shahzad, T. Ion-acoustic wave structures in the fluid ions modeled by higher dimensional generalized Korteweg–de Vries–Zakharov–Kuznetsov equation. *J. Ocean Eng. Sci.* (2022).
11. Zhang, R. F. & Li, M. C. Bilinear residual network method for solving the exactly explicit solutions of nonlinear evolution equations. *Nonlinear Dyn.* **108**(1), 521–531 (2022).
12. Zhang, R. F. & Bilige, S. Bilinear neural network method to obtain the exact analytical solutions of nonlinear partial differential equations and its application to p-gBKP equation. *Nonlinear Dyn.* **95**, 3041–3048 (2019).
13. Zhang, R. F., Li, M. C. & Yin, H. M. Rogue wave solutions and the bright and dark solitons of the (3+ 1)-dimensional Jimbo–Miwa equation. *Nonlinear Dyn.* **103**, 1071–1079 (2021).
14. Zhang, R., Bilige, S. & Chaolu, T. Fractal solitons, arbitrary function solutions, exact periodic wave and breathers for a nonlinear partial differential equation by using bilinear neural network method. *J. Syst. Sci. Complex.* **34**, 122–139 (2021).
15. Zhang, R. F., Li, M. C., Gan, J. Y., Li, Q. & Lan, Z. Z. Novel trial functions and rogue waves of generalized breaking soliton equation via bilinear neural network method. *Chaos Solitons Fractals* **154**, 111692 (2022).
16. Zhang, R. F., Li, M. C., Albishari, M., Zheng, F. C. & Lan, Z. Z. Generalized lump solutions, classical lump solutions and rogue waves of the (2+ 1)-dimensional Caudrey–Dodd–Gibbon–Kotera–Sawada-like equation. *Appl. Math. Comput.* **403**, 126201 (2021).
17. Zhang, R. F., Li, M. C., Cherraf, A. & Vadyala, S. R. The interference wave and the bright and dark soliton for two integro-differential equation by using BNNM. *Nonlinear Dyn.* **111**(9), 8637–8646 (2023).
18. Zhang, R. F., Bilige, S., Liu, J. G. & Li, M. Bright-dark solitons and interaction phenomenon for p-gBKP equation by using bilinear neural network method. *Phys. Scr.* **96**(2), 025224 (2020).
19. Khatun, M. A., Arefin, M. A., Islam, M. Z., Akbar, M. A. & Uddin, M. H. New dynamical soliton propagation of fractional type couple modified equal-width and Boussinesq equations. *Alex. Eng. J.* **61**(12), 9949–9963 (2022).
20. Arefin, M. A., Khatun, M. A., Uddin, M. H. & Inç, M. Investigation of adequate closed form travelling wave solution to the space-time fractional non-linear evolution equations. *J. Ocean Eng. Sci.* **7**(3), 292–303 (2022).
21. Zaman, U. H. M., Arefin, M. A., Akbar, M. A. & Uddin, M. H. Study of the soliton propagation of the fractional nonlinear type evolution equation through a novel technique. *Plos one* **18**(5), e0285178 (2023).
22. Pan, C., Cheemaa, N., Lin, W. & Inc, M. Nonlinear fiber optics with water wave flumes: dynamics of the optical solitons of the derivative nonlinear Schrödinger equation. *Opt. Quantum Electron.* **56**(3), 434 (2024).
23. Seadawy, A. R., Cheemaa, N., Althobaiti, S., Sayed, S. & Biswas, A. Optical soliton perturbation with fractional temporal evolution by extended modified auxiliary equation mapping. *Rev. Mex. Física* **67**(3), 403–414 (2021).
24. Seadawy, A. R. & Cheemaa, N. Improved perturbed nonlinear Schrödinger dynamical equation with type of Kerr law nonlinearity with optical soliton solutions. *Phys. Scr.* **95**(6), 065209 (2020).
25. Seadawy, A. R. & Cheemaa, N. Perturbed nonlinear Schrödinger dynamical wave equation with Kerr media in nonlinear optics via optical solitons. *Int. J. Mod. Phys. B* **34**(10), 2050089 (2020).
26. Cheemaa, N., Seadawy, A. R., Sugati, T. G. & Baleanu, D. Study of the dynamical nonlinear modified Korteweg–de Vries equation arising in plasma physics and its analytical wave solutions. *Results Phys.* **19**, 103480 (2020).
27. Engelbrecht, J., Tamm, K., & Peets, T. On mechanisms of electromechanophysiological interactions between the components of nerve signals in axons. arXiv preprint arXiv:1907.04075 (2019).
28. Bressloff, P. C. Waves in neural media. In *Lecture Notes on Mathematical Modelling in the Life Sciences*. 18–19 (2014).
29. Edelstein-Keshet, L. *Mathematical Models in Biology*. (Society for Industrial and Applied Mathematics, 2005).
30. Engelbrecht, J., Tamm, K. & Peets, T. On mathematical modelling of solitary pulses in cylindrical biomembranes. *Biomech. Model. Mechanobiol.* **14**, 159–167 (2015).
31. Hodgkin, A. L. & Huxley, A. F. Propagation of electrical signals along giant nerve fibres. *Proc. R. Soc. Lond. Ser. B Biol. Sci.* **140**(899), 177–183 (1952).
32. Iqbal, M. S., Seadawy, A. R., Baber, M. Z. & Qasim, M. Application of modified exponential rational function method to Jaulent–Miodek system leading to exact classical solutions. *Chaos Solitons Fractals* **164**, 112600 (2022).
33. Iqbal, M. S., Seadawy, A. R. & Baber, M. Z. Demonstration of unique problems from Soliton solutions to nonlinear Selkov–Schnakenberg system. *Chaos Solitons Fractals* **162**, 112485 (2022).
34. Baber, M. Z., Ahmed, N., Yasin, M. W., Iqbal, M. S., Akgül, A., Riaz, M. B. & Raza, A. Comparative analysis of numerical with optical soliton solutions of stochastic Gross–Pitaevskii equation in dispersive media. *Results Phys.* **44**, 106175 (2023).
35. Shahzad, T., Ahmad, M. O., Baber, M. Z., Ahmed, N., Ali, S. M., Akgül, A., & Eldin, S. M. Extraction of soliton for the confirmable time-fractional nonlinear Sobolev-type equations in semiconductor by $\phi6$-modal expansion method. *Results Phys.* **46**, 106299 (2023).
36. Iqbal, M. S., Seadawy, A. R., Baber, M. Z., Ahmed, N. & Yasin, M. W. Extraction of solitons for time incapable illimitable paraxial wave equation in Kerr-media. *Int. J. Mod. Phys. B* **37**(13), 2350122 (2023).

Acknowledgements

Author contributions

 Conceptualization: Baboucarr Ceesay Data curation: Muhammad Zafarullah baber Formal analysis: Nauman Ahmed and Fuad A. Awwad Validation: Ali Raza and Emad A. A. Ismail Writing-original draft: Muhammad Rafiq and Dilber Uzun Ozsahin Writing-review editing: Hijaz Ahmad. All the authors are agreed to publish this research work.

Funding

Competing interests

The authors declare no competing interests.

Additional information

Correspondence and requests for materials should be addressed to D.U.O.

Reprints and permissions information is available at www.nature.com/reprints.

Publisher's note Springer Nature remains neutral with regard to jurisdictional claims in published maps and institutional affiliations.